**Young S. Shin**
**James E. Chisum**
*Mechanical Engineering Department*
*Naval Postgraduate School*
*Monterey, CA 93943-5107*

# Modeling and Simulation of Underwater Shock Problems Using a Coupled Lagrangian–Eulerian Analysis Approach

*The application of coupled Lagrangian–Eulerian analysis to various types of underwater shock problems was investigated, with the verification and validation of this analysis approach in mind. Analyses were conducted for a simple TNT detonation problem and for the classical problems of an infinite cylindrical shell and a spherical shell loaded by a plane acoustic step wave. The advantages, disadvantages, and limitations of this approach are identified and discussed.* © *1997 John Wiley & Sons, Inc.*

## INTRODUCTION

The modeling and simulation of the response of marine structures (surface ships, submarines, etc.) to underwater explosions requires an understanding of many different subject areas. These include the process of underwater explosion events, shock wave propagation, explosion gas bubble behavior and bubble-pulse loading, bulk and local cavitation, linear and nonlinear structural dynamics, and fluid–structure interaction (Shin and Geers, 1995). This article describes efforts to apply coupled Lagrangian–Eulerian finite element analysis techniques to several simple underwater shock problems.

When an underwater explosion occurs far away from the target structure, a boundary element approach such as the doubly asymptotic approximation (DAA) (Geers, 1971, 1978; Geers and Fellipa, 1983) is very useful for shock response calculation. The DAA approach models the acoustic 3-dimensional fluid medium surrounding the structure as a 2-dimensional membrane covering the wet surface of the structure. The major advantage of the DAA is that it models the interaction of the structure and the surrounding acoustic fluid medium in terms of wet-surface response variables only, eliminating the need to model the fluid volume elements surrounding the structure.

However, for certain classes of problems DAA techniques have not been advanced to the point that they can provide useful results. This is particularly true for the case when an underwater explosion occurs close to the target structure. In this case, not only is the nonacoustic incident shock wave propagation important, but the explosion gas bubble motion also plays an important role. The pressure pulsation produced by such explosion gas

Received January 15, 1995; Accepted September 4, 1996.
Shock and Vibration, Vol. 4, No. 1, pp. 1–10 (1997)

CCC 1070-9622/97/01001-10

bubbles can, under certain circumstances, produce significant whipping of nearby marine structures.

In addition, there are certain practical constraints on the ability to conduct experimentation to determine structural responses to underwater explosions. Full-scale experimentation is extremely expensive, and certain physical phenomena related to these explosions cannot be scaled in a practical experimental setup.

In light of these factors, a more basic approach might allow the solution of heretofore unsolvable problems. In this approach, each material in an underwater shock problem is modeled in the most advantageous way for that class of material: fluid media and explosives using Eulerian elements, and structural materials using Lagrangian elements. This approach is becoming practical for underwater explosion problems for two reasons. First, the ongoing advances in computer capabilities has made significant computational resources available for most workers. Second, advanced finite element programs that can efficiently calculate the fluid–structure interaction between Eulerian and Lagrangian materials and that are capable of dealing with several different Eulerian materials in the same problem have recently become available.

On advantage of this approach is that there are few approximations involved, the resulting solution can essentially be made as accurate as the discretization allowed by the available computational resources and the certainty with which the properties of the materials involved are known will permit. This approach also overcomes the problems involved with modeling of all the material in a problem with Lagrangian elements, which in an underwater shock problem quickly become so distorted that the stable time step size approaches zero and the time to compute a solution out to near steady state approaches infinity. Neither is the approach of modeling all of the material in an underwater shock problem using Eulerian materials generally practical, as this approach requires that an extremely large number of Eulerian elements be used in order to accurately capture the response of structural materials in the problem, which is usually the primary item of interest.

By using a finite element code that contains both Lagrangian and Eulerian processors and a method for computing the fluid–structure interaction at the interface between Lagrangian and Eulerian materials, the advantages of both types of analysis are realized and the shortcomings associated with attempting to use one or the other alone are eliminated. This is the approach we chose to pursue for various types of underwater shock problems, including the analyses described in this article, that were undertaken with verification and validation of this analysis approach in mind.

## NUMERICAL COMPUTER CODE

The coupled Lagrangian–Eulerian finite element analysis program used for the results described here was MSC/Dytran (1995). This program was developed by combining and extending two other computer programs: MSC/Dyna (1991) as the Lagrangian processor and MSC/Pisces (1991) as the Eulerian processor. Both of these programs have a proven record in the analysis areas for which they were developed.

Like MSC/Dyna, MSC/Dytran is capable of handling nonlinear, large strain structural response problems. MSC: Dytran is also capable of solving problems involving Lagrangian–Lagrangian two surface (contact–impact) and single surface (folding) problems. A complete constitutive model can be defined in terms of an equation of state, a shear model, a yield model, a failure model, and a spall model.

The multimaterial Eulerian processor in MSC/Dytran allows up to nine different Eulerian materials to be present in a given problem. In addition, two different methods are available to provide for calculation of the fluid–structure interaction between Lagrangian and Eulerian materials.

In the "general coupling" method, the Lagrangian and Eulerian meshes are geometrically independent and interact via a coupling surface attached to the Lagrangian structure. This method requires that the coupling surface form a closed, simply connected volume, on one side (inside or outside) of which the Eulerian elements are "void" (contain no material). The deformable coupling surface "cuts across" Eulerian elements, changing their control volume and surface areas. To prevent the stable time step size from being controlled by very small Eulerian control volumes formed by the coupling surface, elements for which the ratio between the "covered" (void) volume fraction and the initial volume is less than a user modifiable "blend" parameter are combined with adjacent elements to form larger elements.

The other method provided by MSC/Dytran for coupling of Lagrangian and Eulerian materials is arbitrary Lagrange–Euler coupling. In this method, the fluid and structural mesh geometries are not independent. Instead, the interface surface

between the Lagrangian and Eulerian elements is actually composed of the union of the faces of these elements. As this interface is deformed during deformation of the Lagrangian structure, Eulerian grid points that are attached to this also move. To keep the geometry of the Eulerian mesh relatively "nice," other Eulerian grid points away from the coupling surface can be allowed to move, e.g., toward the center of their nearest neighbors. In this method, the Eulerian mesh is not stationary. However, the motion of the Eulerian mesh is purely geometrical; the velocity of material through this mesh is independent of the motion of the mesh.

## TNT DETONATION

A 10-cm long slab of cast TNT is detonated along one end. The TNT is assumed to behave as a Jones–Wilkins–Lee (JWL) high explosive. The JWL equation of state is expressed as follows (Dobratz, 1981):

$$p = A\left(1 - \frac{\omega\eta}{R_1}\right)e^{-(R_1/\eta)} + B\left(1 - \frac{\omega\eta}{R_2}\right)e^{-(R_2/\eta)} + \omega\eta\rho_0 E, \tag{1}$$

where the parameters for TNT are $A = 3.712 \times 10^{11}$ Pa, $R_1 = 4.15$, $B = 0.0321 \times 10^{11}$ Pa, $R_2 = 0.95$, $\omega = 0.30$, $\eta = \rho/\rho_0$, $\rho$ is the overall material density, $\rho_0 = 1630$ kg/m$^3$ (reference density), $E = 4.29 \times 10^6$ J/kg (specific internal energy per unit mass), and an experimentally determined detonation velocity of 6930 m/s is used for TNT. The LLNL Explosives Handbook cautions that the JWL state equation is valid only for "large charges" (Dobratz, 1981); this ensures that it is only used to model explosions for which high-order detonation occurs.

A 1-dimensional Eulerian model was used for this problem, as a plane detonation front is assumed. Analyses were conducted using 125, 250, 500, 1000, and 2000 elements to illustrate the effects of discretization in this problem. The dimensions of the hexahedron Eulerian elements were $0.1 \times 0.1 \times 0.8$, 0.4, 0.2, 0.1, and 0.05 mm, respectively. Wall boundary conditions (no material transport across the boundary) were used everywhere, including the last face of the last element (at 10 cm), because the analyses were terminated before the detonation front reached this point. Detonation was initiated at time $t = 0$.

The results are shown in Figs. 1 and 2. Figure 1 shows the pressure as a function of the distance along the slab at 1-$\mu$s intervals from 1 through 14 $\mu$s for the 2000 element model. Figure 2 illustrates the effect of increasing the number of elements on both the peak pressure at a given location and the "sharpness" of typical pressure profiles in space. Peak pressures at 1-$\mu$s intervals are shown, along with complete pressure profiles at 7 and 14 $\mu$s.

The dashed line in these figures represents the experimentally determined Chapman–Jouguet detonation pressure, which is the pressure at the equilibrium plane at the trailing edge of the very thin chemical reaction zone (Dobratz, 1981). This pressure is determined in theory by intersecting the TNT Hugonoit curve [allowable final ($p$, $\rho$) states, from conservation of energy] with the Rayleigh line [allowable final ($p$, $\rho$) states, from conservation of mass and momentum], where the slope of the Rayleigh line is determined by the Chapman–Jouguet condition that the detonation velocity is the minimum velocity for which the Rayleigh line intersects the Hugonoit (Cole, 1948).

In this problem, the experimentally determined detonation velocity for TNT was used; hence the calculated peak pressure should (and did) converge to the experimentally determined Chapman–Jouguet detonation pressure. The results are quite acceptable if it is taken into consideration that MSC/Dytran is a first-order code that smears the shock front over several elements (always conserving mass, momentum, and energy), resulting in a decrease in peak shock wave pressure (MSC/Dytran, 1995).

## COUPLED ANALYSIS OF CLASSICAL PROBLEMS

To examine the performance of using coupled Lagrangian–Eulerian finite element analysis for underwater shock problems, two classical problems for which analytical solutions are available were analyzed. These analyses examined the elastic response of a spherical shell and an infinite cylinder to loading from a plane acoustic step wave propagating through an acoustic fluid media.

Huang (1969, 1970) solved these problems analytically, using a direct inverse Laplace transform of a finite number of terms of the infinite series expansion of the equations for the respective shells. For our finite element analyses, the same material properties, parameters, and nondimen-

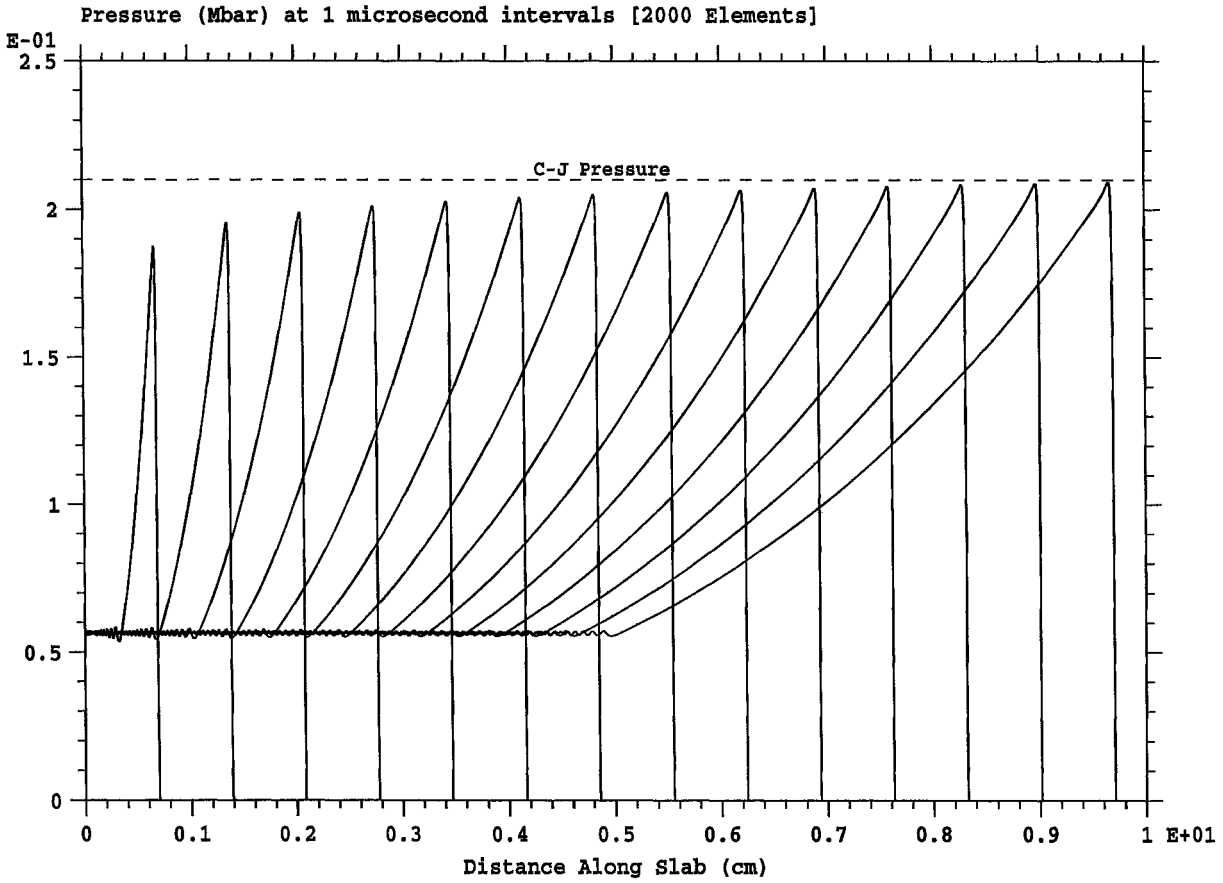


**FIGURE 1** TNT detonation pressure profiles at 1-$\mu$s intevals.

sionalization procedures used by Huang in his analyses were utilized.

## Spherical Shell Subjected to a Plane Acoustic Step Wave

Figure 3 shows the geometry of the spherical shell subjected to a plane acoustic step wave problem. The material properties and parameters used for this problem were:

1. shell material, steel;
2. Young's modulus for steel, $30 \times 10^6$ psi;
3. Poisson's ratio for steel, 0.3;
4. density of steel, 486 lb m/ft$^3$;
5. shell thickness to radius radio, 0.02;
6. fluid, Water;
7. water density, 62.4 lb m/ft$^3$;
8. water acoustic wave speed, 4794 ft/s.

The problem was nondimensionalized using the radius of the sphere as the characteristic length, the time for an acoustic wave to transit one radius as the characteristic time, and the bulk modulus of water as the characteristic pressure. A bulk modulus equation of state was used to model the water in this problem as shown in the equation below:

$$p(\rho) = \rho_0 c^2 \left( \frac{\rho}{\rho_0} - 1 \right), \tag{2}$$

where $p$ is the pressure, $c$ is the acoustic velocity in the water, $\rho_0$ is the reference water density, and $\rho$ is the water density. A small incident pressure wave magnitude ($1 \times 10^{-3}$ bulk modulus units) was used to keep deformations small enough for the elastic assumption to be valid.

For our finite element model, a quarter symmetry model was used. An elastic material model consisting of 150 quadrilateral Lagrangian shell elements was used to model one-quarter of the spherical steel shell. A single constraint set was used to constrain the appropriate translational and rotational degrees of freedom of grid points lying on symmetry planes.

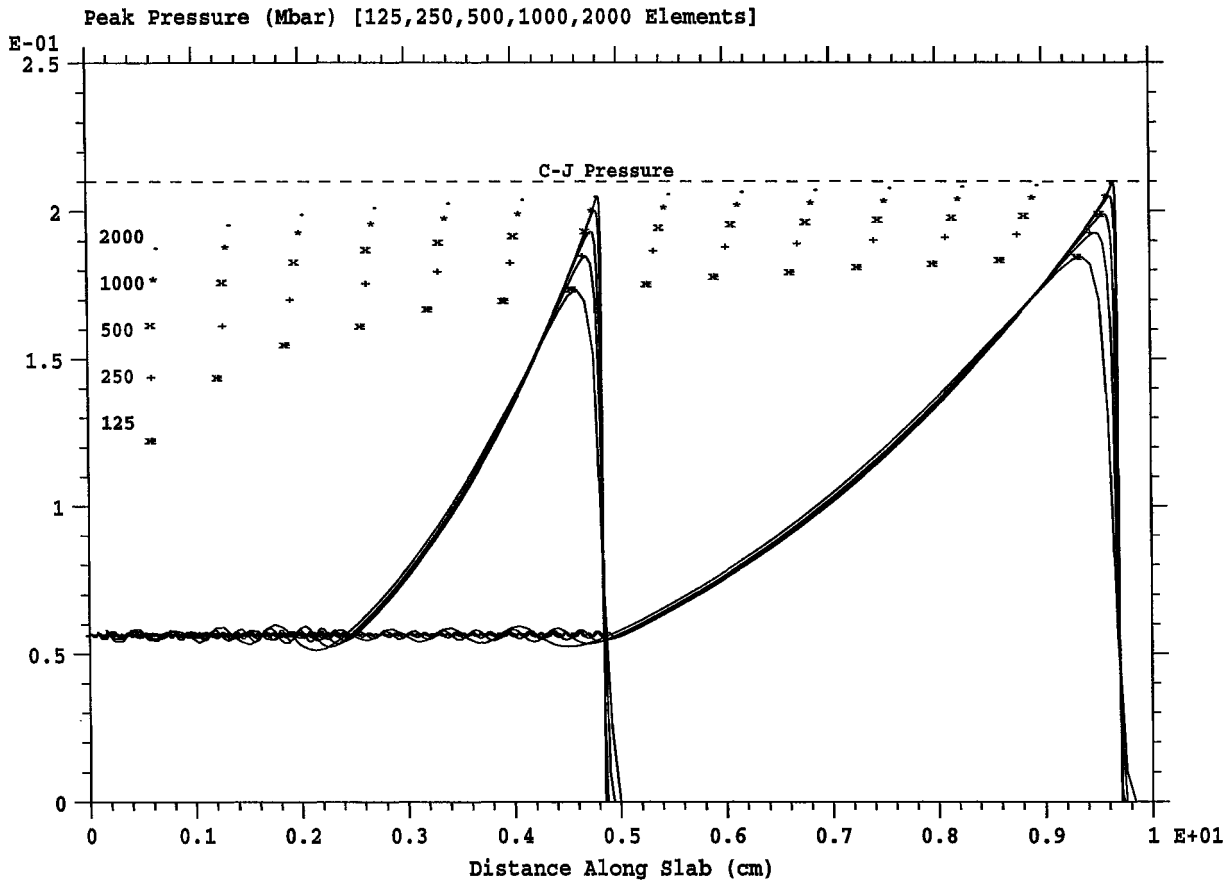


**FIGURE 2** TNT detonation peak pressures for various model discretizations.

MSC/Dytran's general coupling fluid–structure interaction method, in which the Lagrangian and Eulerian meshes are independent and interact via a coupling surface, was used for this problem. This method requires that the coupling surface form a closed, simply connected volume; for simplicity, this closed volume was generated by using 450 dummy elements in addition to the 150 Lagrangian shell elements used to model the steel shell. The Lagrangian (steel) shell elements, the dummy elements, and the resulting closed coupling surface are illustrated in Fig. 4.

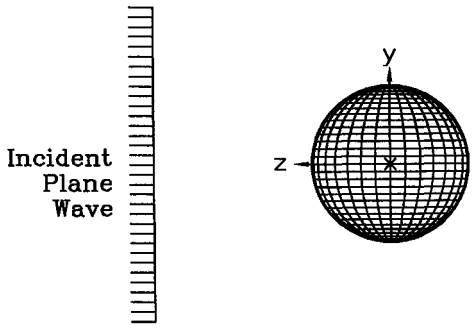


**FIGURE 3** Spherical shell subjected to plane step wave problem geometry.

Because only a finite volume of fluid material can be modeled using this approach, it was decided to construct a model for which the solution would be unaffected by reflection from the boundaries of the fluid volume for times less than 6 radius transit times. The block of water modeled is thus a rectangle bounded by the planes $x = 0$ and $x = 4$, $y = 0$ $y = 4$, and $z = 4$ and $z = 4$, where the point (0, 0, 0) represents the center of the sphere and units are in terms of the radius of the sphere. Every point on the shell is thus at least 3 radii away from a boundary; and because acoustic waves travel 1 shell radius transit time, no boundary reflection reaches the shell for 6 radius transit times. The fluid mesh used consists of 65,536 cubical Eulerian elements; the length of each side of each element is 1/8 radius.

All boundaries of this fluid volume were left with a "wall" boundary condition (no material

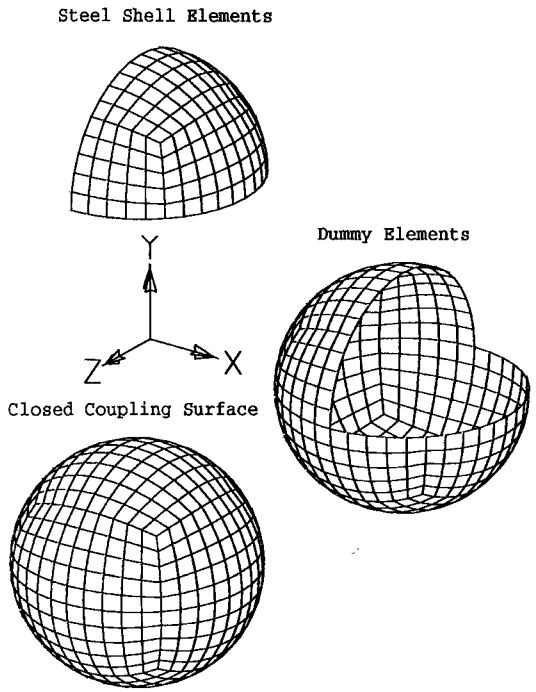


**FIGURE 4** Lagrangian shell elements, dummy elements, and the resulting closed coupling surface for the spherical shell/plane step wave problem.

transport across boundary) except the boundary at $z = 4$ radii; this boundary was given a "flow" boundary condition, with a pressure ($p$) of 0.001 bulk modulus and a particle velocity ($u$), determined from the 1-dimensional wave equation

$$p = \rho c u, \tag{3}$$

of 0.001 times the acoustic wave speed ($c$) in water in the $-z$ direction. Initial conditions were imposed on all of the Eulerian elements such that all elements between the $z = 4$ radii and $z = 1$ radius planes had an initial pressure of 0.001 bulk modulus and a particle velocity of 0.001 times the acoustic wave speed in water in the $-z$ direction, and all elements between the $z = 1$ and $z = -4$ radii planes had zero initial pressure and particle velocity. Time $t = 0$ for the finite element analysis thus corresponds to the instant when the plane step wave first touches the sphere at the point (0, 0, 1).

The relationship between the size of the spherical shell and the fluid volume modeled in this problem is illustrated in Fig. 5, from two different viewpoints. For clarity, only the outline of the fluid block that was modeled is shown.

The resulting transient solution for the radial velocity of the shell, at azimuth angles of 0°, 90°, and 180° [which correspond to the points (0, 0, 1), (0, 1, 0), and (0, 0, −1), using the coordinate system shown in Fig. 5] are shown in Fig. 6. Huang and Mair's (1996) new 70 term Cesaro sum solution for these same points is shown for comparison purposes. While our finite element solution shows some overshoot and resulting oscillation at 0°, in general the agreement with Huang's analytical solution is quite good. All velocities in Fig. 6 are nondimensionalized to be independent of the magnitude of the incident pressure wave, by dividing the original nondimensional velocity by the nondimensional magnitude of the incident pressure wave.

## Infinite Cylinder Subjected to a Plane Acoustic Step Wave

Figure 7 shows the geometry of the infinite cylinder subjected to a plane acoustic step wave. The

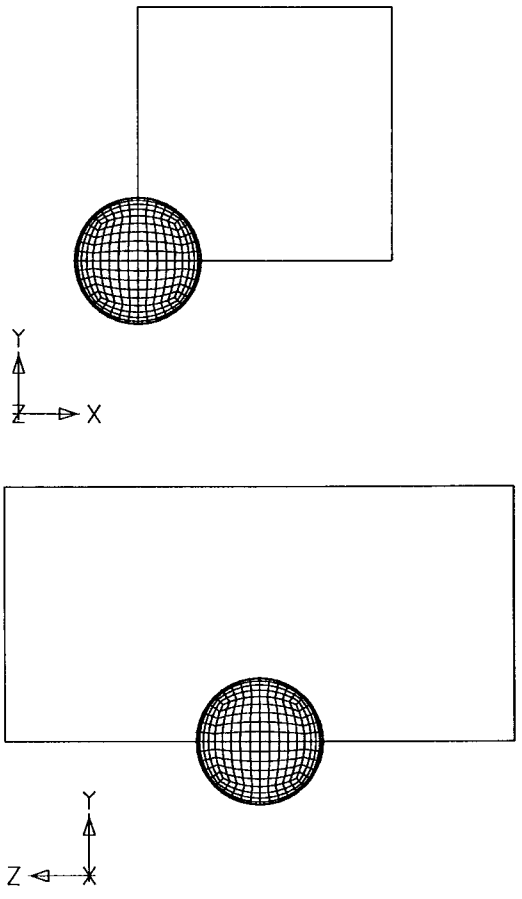


**FIGURE 5** Size and position of the spherical shell relative to the Eulerian fluid volume for the spherical shell/plane step wave problem.

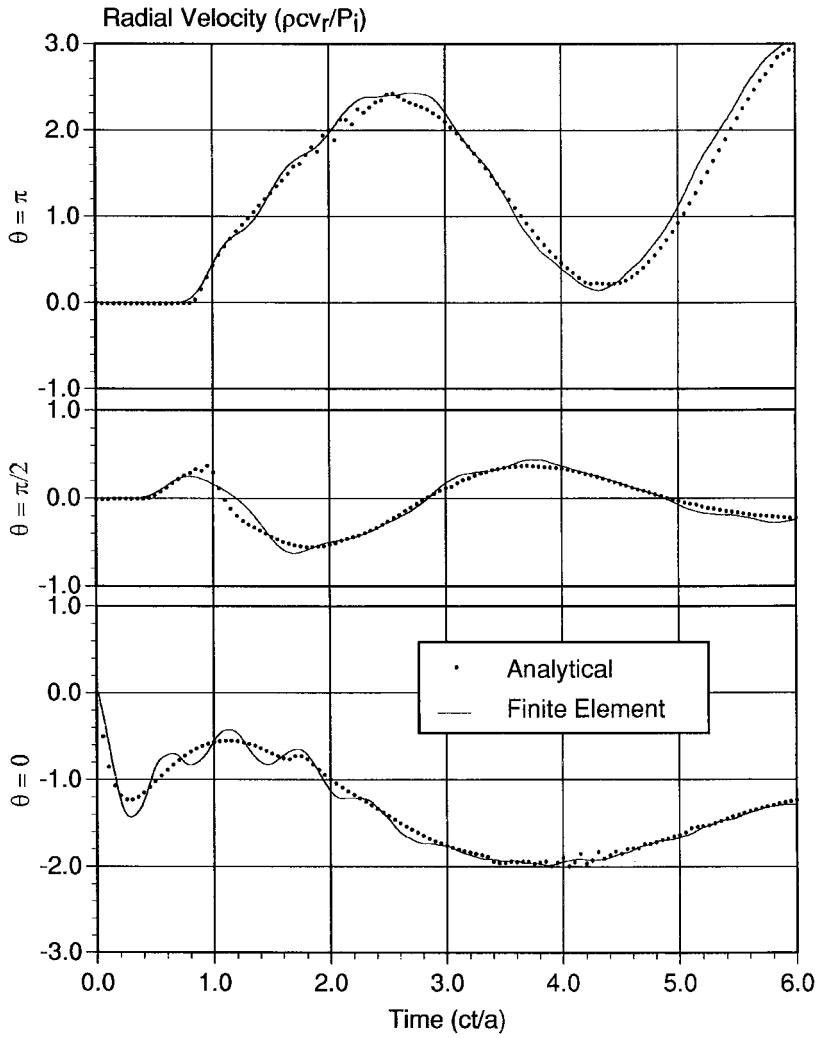


**FIGURE 6** Nondimensional radial velocity vs. nondimensional time for the spherical shell/plane step wave problem.

same material properties, parameters, and nondimensionalization procedures used in the spherical shell problem were used for this problem, except that a shell thickness to radius ratio of 0.029056 was used for this problem.

Because of the symmetry of the problem, only a single 0.1 cylinder radius wide "ring" of the infinite cylinder was modeled for our finite element analysis. In addition, because the problem has symmetry about the plane defined by a point on the axis of the cylinder and the vector normal to the incoming pressure wave front, only one-half of this ring was modeled.

The shell was modeled with 36 Lagrangian elements, with appropriate translational and rotational symmetry constraints placed upon the grid points associated with these elements. MSC/Dy-

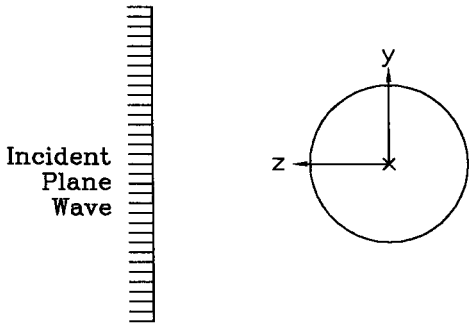


**FIGURE 7** Infinite cylinder subjected to plane step wave problem geometry.

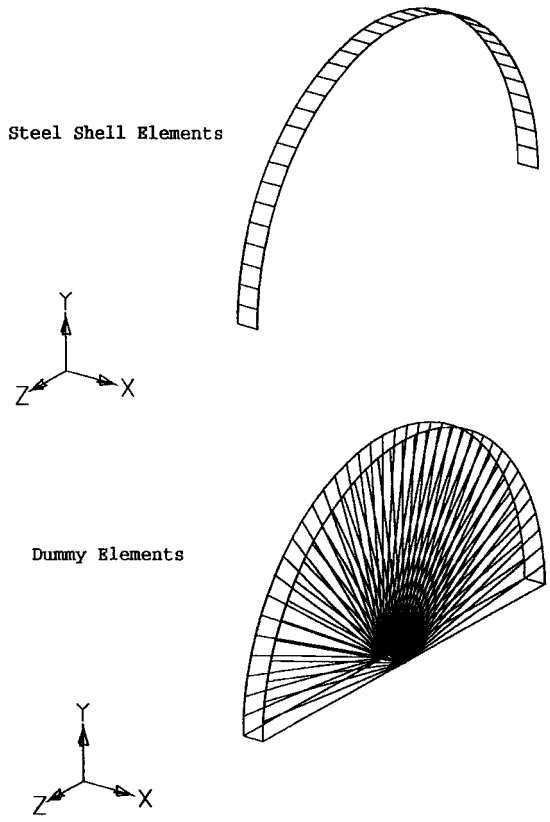


**FIGURE 8** Lagrangian shell elements and dummy elements for the infinite cylinder/plane step wave problem.

tran's general coupling fluid–structure interaction method was used for this problem; to form the closed volume coupling surface required for this method, 72 dummy triangular and two dummy quadrilateral elements were defined. Figure 8 shows the Lagrangian structural elements and dummy elements used in our finite element model for this problem.

The fluid mesh used for this problem consisted of a thin block of elements with dimensions of $0.1 \times 4 \times 8$ cylinder radii. This fluid block was meshed with $1 \times 88 \times 176$ hexahedron elements, for a total of 15,488 fluid elements. Thus, the length of each element in the $y$ and $z$ directions was 1/11 cylinder radius. As in the spherical shell problem, the amount of fluid modeled is sufficient to prevent reflection of acoustic waves from the boundaries from affecting the solution for times less than 6 radius transit times.

All boundary conditions for the fluid mesh shown were left as wall (no flow) boundaries, except for the boundary at $a = 4$ cylinder radii, which was given a flow boundary condition with a prescribed pressure of 0.001 bulk modulus and a $z$-direction particle velocity of $-0.001$ cylinder radius/cylinder radius transit time. Initial conditions were prescribed such that all fluid between the $z = 4$ and 1 cylinder radii planes had these same values, and the remaining fluid had zero initial pressure and particle velocity. Thus, time $t = 0$ corresponds to the instant when the pressure wave just touches the cylinder at the point (0, 0, 1) (using the rectangular coordinates of Fig. 8; in cylindrical coordinates this point is at a radius of 1 cylinder radius from the cylinder axis, at an angle of 0°).

The size and position of the cylinder relative to the fluid volume modeled is illustrated in Fig. 9. Only the outline of the fluid volume modeled is shown in this figure.

Results from our analysis for the pressure-independent nondimensional radial velocity of the shell at 0°, 90°, and 180° are compared in Fig. 10 with the 8-term finite series analytical solution found by Huang (1970). Again, very good

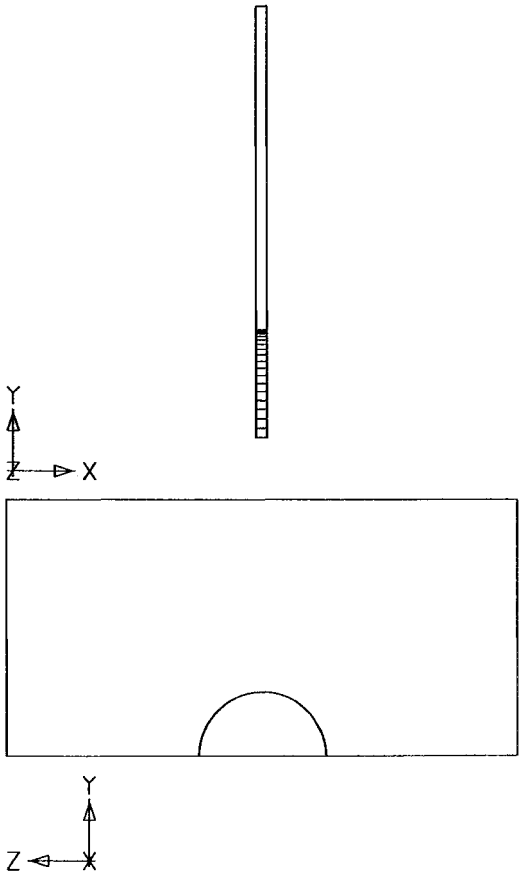


**FIGURE 9** Size and position of infinite cylinder model relative to the Eulerian fluid volume for the infinite cylinder/plane step wave problem.

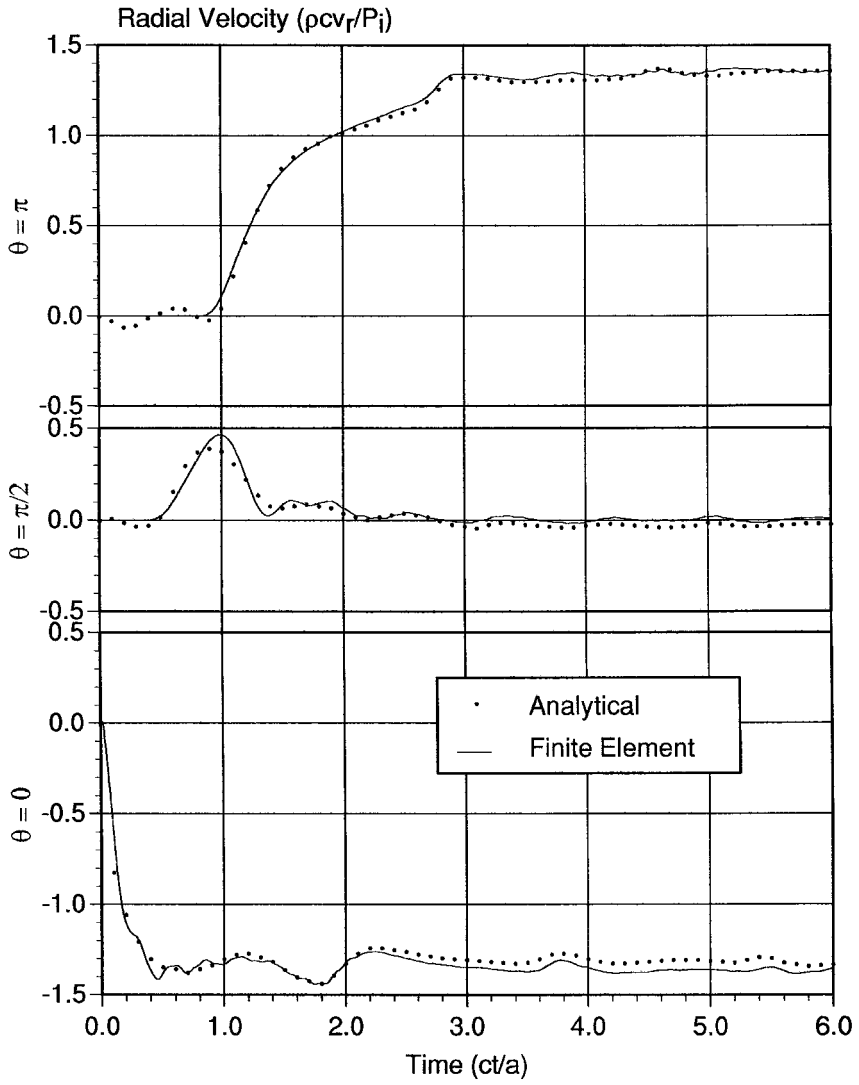


**FIGURE 10** Nondimensional radial velocity vs. nondimensional time for the infinite cylinder/plane step wave problem.

agreement between the finite element and analytical solutions is seen.

## CONCLUSION

This article describes analysis procedures used in and results obtained by directly applying coupled Lagrangian–Eulerian finite element analysis to several underwater shock problems. The problem types analyzed encompass the explosive detonation process, classical acoustic wave–shell fluid–structure interaction, and explosion gas bubble motion.

The TNT detonation process modeled using a JWL equation of state simulates the explosion physics relatively well, the calculated pressure converging to the Chapman–Jouguet detonation pressure. The results for the acoustic wave–shell fluid–structure interaction problems compare quite well with the analytical solutions for these problems.

One of the benefit of the direct finite element method used is that it does not rely on time or frequency domain approximations, so that the solution accuracy obtained is dependent only upon the fineness of the mesh used and the accuracy with which the equation of state parameters for

**Table 1. Execution Summary**

| Problem Description | Memory Used (Words) | Run Time (min) |
|---|---|---|
| TNT detonation | | |
| 125 elements | 28,998 | 0.49 |
| 250 elements | 57,873 | 0.86 |
| 500 elements | 115,623 | 1.60 |
| 1000 elements | 231,123 | 3.05 |
| 2000 elements | 462,123 | 11.15 |
| Spherical shell/plane step wave | 10,503,223 | 134.12 |
| Infinite cylinder/plane step wave | 2,797,030 | 25.16 |

the modeled materials are known. This method does involve a far greater number of elements than a boundary element method; however, the ever expanding capability of computers makes direct application of the finite element method using coupled Lagrangian–Eulerian and multimaterial Eulerian analysis practical for an increasing number of problems. Reasonable problem solution times can be obtained because time marching using an explicit finite difference technique can be very efficient, even for very large problems (no eigenvalue problem need be solved).

All of the problems described here were analyzed on a 32 MFLOP (millions of floating point operations per second) IBM RS/6000 Model 560 workstation with 64 megabytes of RAM (random access memory). This is a moderately capable platform; many researchers now have access to equivalent or more powerful workstations. Table 1 summarizes the memory required for these analyses, along with the total execution time (including the time required for problem generation and input/output).

Besides the obvious factors of number of elements, element size, and number of time steps required to reach the solution end time, our experience has shown that execution times are significantly effected by whether or not the analysis can be done within the available physical RAM. Run times are appreciably increased if the problem has to use "virtual memory" (hard disk space set aside for swapping information when the computer is out of physical RAM).

## REFERENCES


Cole, R. H., 1948, *Underwater Explosions,* Princeton University Press, Princeton, NJ.

Dobratz, B. M., 1981, "LLNL Explosives Handbook," UCRL-52997, Lawrence Livermore National Laboratory, Livermore, CA, pp. 8-21–8-23.

Geers, T. L., 1971, "Residual Potential and Approximate Methods for Three-Dimensional Fluid–Structure Interaction Problems," *Journal of the Acoustical Society of America,* Vol. 49, pp. 1505–1510.

Geers, T. L., 1978, "Doubly Asymptotic Approximations for Transient Motions of Submerged Structures," *Journal of the Acoustical Society of America,* Vol. 64, pp. 1152–1159.

Geers, T. L., and Fellipa, C. A., 1983, "Doubly Asymptotic Approximations for Vibration Analysis of Submerged Structures," *Journal of the Acoustical Society of America,* Vol. 73, pp. 1500–1508.

Huang, H., 1969, "Transient Interaction of Plane Acoustic Waves with a Spherical Elastic Shell," *Journal of the Acoustical Society of America,* Vol. 45, pp. 661–670.

Huang, H., 1970, "An Exact Analysis of the Transient Interaction of Acoustic Plane Waves with a Cylindrical Elastic Shell," *ASME Journal of Applied Mechanics,* pp. 1091–1099.

Huang, H., and Mair, H. U., 1996, "Neoclassical Solution of Transient Interaction of Plane Acoustic Waves with a Spherical Elastic Shell," *Shock and Vibration,* Vol. 3, pp. 85–98.

MacNeal–Schwendler Corporation, *MSC/Dyna User's Manual,* 1991, Los Angeles, CA.

MacNeal–Schwendler Corporation, *MSC/Dytran User's Manual,* 1995, Los Angeles, CA.

The MacNeal-Schwendler Corporation, *MSC/Pisces 2DELK User's/Theoretical Manual,* 1991, Los Angeles, CA.

Shin, Y. S., and Geers, T. L., 1995, "Response of Marine Structure to Underwater Explosions," International Short Course Notebook, Shock and Vibration Research, Monterey, CA.